guez, N. D. Sze, *Nature (London)* **322**, 811 (1986); J. D. Mahlman and S. B. Fels, *Geophys. Res. Lett.* **13**, 1316 (1986); L. B. Callis and M. Natarajan, *J. Geophys. Res.* **91**, 10771 (1986).
2. J. C. Farman, B. G. Gardiner, J. D. Shanklin, *Nature (London)* **315**, 207 (1985).
3. S. Solomon *et al.*, *ibid.* **321**, 755 (1986).
4. M. B. McElroy, R. J. Salawitch, S. C. Wofsy, J. A. Logan, *ibid.*, p. 759.
5. L. T. Molina and M. J. Molina, *J. Phys. Chem.* **91**, 433 (1987).
6. M. B. McElroy, R. J. Salawitch, S. C. Wofsy, *Geophys. Res. Lett.* **13**, 1296 (1986).
7. P. J. Crutzen and F. Arnold, *Nature (London)* **324**, 651 (1986); O. B. Toon, P. Hamill, R. P. Turco, J. Pinto, *Geophys. Res. Lett.* **13**, 1284 (1986).
8. H. M. Steele, P. Hamill, M. P. McCormick, T. J. Swissler, *J. Atmos. Sci.* **40**, 2055 (1983).
9. M. J. Rossi, R. Malhotra, D. M. Golden, *Geophys. Res. Lett.* **14**, 127 (1987).
10. A. C. Baldwin and D. M. Golden, *Science* **206**, 562 (1979).
11. D. M. Golden, G. N. Spokes, S. W. Benson, *Angew. Chem. Int. Ed. Engl.* **12**, 534 (1973).
12. The sticking coefficient is given by

$$\gamma = (A_h/A_s)[(I^0 - I)/I]$$

where A_h and A_s are the area of the Knudsen cell escape aperture and the surface area of the copper block, respectively, and I^0 and I are the $ClONO_2$ mass spectrometer signals in the absence and presence of the surface, respectively (*11*). The present value of γ was obtained with *m/e* 46 rather than *m/e* 30 to achieve higher sensitivity. The mass peak *m/e* 51 could not be used to calculate γ due to interference from Cl_2O formed in a secondary reaction.
13. This determination of γ assumes that the surface area of the ice is identical to that of the copper block. The true surface area could be larger because of the microscopic structure of the ice. To the extent that we have underestimated the ice surface area, our value of γ represents an upper limit.
14. A referee has suggested that Cl_2O can be formed by the reaction

$$HOCl + ClONO_2 \rightarrow Cl_2O + HNO_3$$

This reaction in combination with reaction 1 yields the stoichiometry given by reaction 3. We make no implications as to the detailed mechanism.
15. L. T. Molina and M. J. Molina, *J. Phys. Chem.* **82**, 241 (1978); H. D. Knauth, H. Alberti, H. Clausen, *ibid.* **83**, 1604 (1979).
16. C. L. Lin, *J. Chem. Eng. Data* **21**, 411 (1976).
17. M. A. Tolbert, unpublished results.
18. R. R. Friedl, J. H. Goble, S. P. Sander, *Geophys. Res. Lett.* **13**, 1351 (1986).
19. M. J. Molina, T. L. Tso, L. T. Molina, F. C. Y. Wang, *Science* **238**, 1253 (1987).
20. We thank R. T. Rewick for assistance in the synthesis of $ClONO_2$. Funding for this work was provided by the National Science Foundation under grant ATM-8600764 and by the National Aeronautics and Space Administration under contract No. NASW-3888.

5 October 1987; accepted 27 October 1987

Spacelab-2 Plasma Depletion Experiments for Ionospheric and Radio Astronomical Studies

M. MENDILLO, J. BAUMGARDNER, D. P. ALLEN, J. FOSTER, J. HOLT, G. R. A. ELLIS, A. KLEKOCIUK, G. REBER

The Spacelab-2 Plasma Depletion Experiments were a series of studies to examine shuttle-induced perturbations in the ionosphere and their application to ground-based radio astronomy. The space shuttle Challenger fired its orbital maneuvering subsystem engines on 30 July and 5 August 1985, releasing large amounts of exhaust molecules (water, hydrogen, and carbon dioxide) that caused the electrons and ions in Earth's upper atmosphere to chemically recombine, thereby creating so-called "ionospheric holes." Two burns conducted over New England produced ionospheric peak depletions ranging from 25 to 50 percent, affected the ionosphere over a 200-kilometer altitude range, and covered 1° to 2° of latitude. Optical emissions associated with the hole spanned an area of several hundred thousand square kilometers. A third burn was conducted over a low-frequency radio observatory in Hobart, Australia, to create an "artificial window" for ground-based observations at frequencies normally below the natural ionospheric cutoff (penetration) frequency. The Hobart experiment succeeded in making high-resolution observations at 1.7 megahertz through the induced ionospheric hole.

THE SPACELAB-2 PLASMA DEPLETION Experiments conducted by the space shuttle Challenger from 29 July to 5 August 1985 represented an innovative use of the shuttle to perform space physics experiments in Earth orbit. For the first time in the shuttle program, the orbiter's small onboard engines (called the Orbital Maneuvering Subsystem or OMS engines) were fired for reasons other than to change the shuttle's orbit. These scientifically dedicated OMS firings were used to conduct a series of "active space plasma experiments" in which large quantities of neutral gases were injected into the ionosphere.

The OMS exhaust gases (H_2O, H_2, and CO_2) react rapidly with the ambient ionospheric plasma, causing the dominant atomic ions (O^+) to be converted to molecular ions (H_2O^+, OH^+, and O_2^+), which then recombine very rapidly with the ambient electrons (e^-) to form neutral species that yield optical emissions. The end result is to cause a sudden depletion in the local plasma concentrations, the creation of a so-called "ionospheric hole" (*1–3*).

The reasons for introducing such a well-defined stress into the ionosphere fall into three broad areas: (i) All shuttle missions use OMS burns for orbit insertion, for changes of orbit during a mission, and for deorbit. The prediction that ionospheric holes occur with each such maneuver needed to be verified for operational and environmental reasons. (ii) The creation of an ionospheric hole, performed in conjunction with a multidiagnostic observing program, allows one to study the "system response function" of the upper atmosphere. Earth's plasma environment involves a complex mix of processes linking solar ionizing radiation, chemical reactions between many ionized and neutral components of the atmosphere, dynamic properties (for example, winds and diffusion) of the upper atmosphere, and electrodynamic processes imposed by electric and magnetic fields of terrestrial and solar wind origin. By introducing known perturbations into a well-defined subsystem and measuring the response, we can apply standard laboratory techniques to Earth's plasma environment. Such input-output tests, coupled to computer models of the overall system, form the essence of what is meant by the phrase "active experiments" in space. (iii) Artificially induced plasma depletions, once understood and capable of being modeled in detail, can then be used to instigate other space plasma phenomena, such as the growth of plasma instabilities or the modification of radio propagation paths, thus introducing a second level of laboratory-in-space experimentation to the space sciences (*4*).

The concept behind using a Spacelab mission to investigate both the basic plasma physics and applications areas of ionospheric holes was that a shuttle mission dedicated completely to space science had the unique ability to control all aspects of the vehicle's orbit. This requirement was of crucial importance because ionospheric holes are effects left literally in the wake of the shuttle, and thus all major observations had to be made from well-equipped ground-based observatories. The OMS burns had to be conducted at certain altitudes, with precise ground tracks, and within certain local time windows and specified lunar lighting conditions.

The burns for the three experiments (Millstone 1, Millstone 2, and Hobart) are

M. Mendillo, J. Baumgardner, D. P. Allen, Department of Astronomy, Boston University, Boston, MA 02215. J. Foster and J. Holt, Massachusetts Institute of Technology, Haystack Observatory, Westford, MA 01886. G. R. A. Ellis, A. Klekociuk, G. Reber, Department of Physics, University of Tasmania, Hobart, Tasmania, Australia.

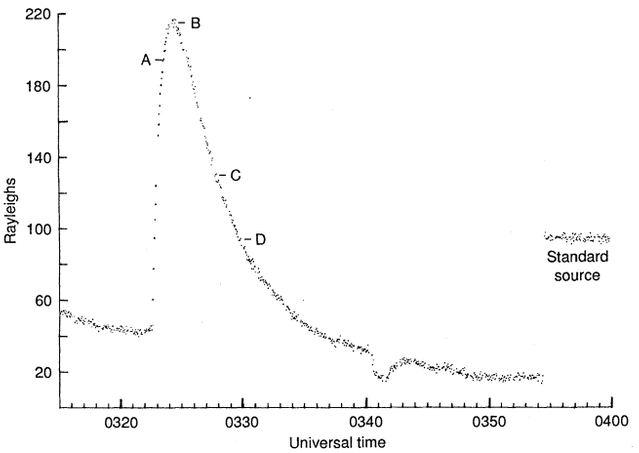

Fig. 1. Airglow observations at 6300 Å obtained with a 1° photometer at Horton Point, Long Island, pointed toward the center of the Millstone Hill nighttime OMS burn experiment on 30 July 1985. The points marked (A) through (D) indicate the times for simultaneous imaging results shown in Fig. 2 and are as follows: A, 0323:33 UT; B, 0325:02 UT; C, 0328:00 UT; and D, 0329:50 UT.

named by the major radio observatory associated with each experiment. The Millstone Hill Incoherent Scatter Radar is part of the Massachusetts Institute of Technology Haystack Observatory in Westford, Massachusetts (42.62°N, 70.48°W). An incoherent scatter radar is one of the major observational tools for ionospheric physics (*5*). Pulsed ultrahigh-frequency transmissions returned from the ionosphere provide line-of-sight observations of the local electron and ion densities, their temperatures, and the overall bulk plasma drift. Separate nighttime (Millstone 1) and daytime (Millstone 2) OMS burns were conducted to investigate the formation and evolution of ionospheric depletions under significantly different conditions. The nighttime experiment used a 47-second OMS burn (during which the shuttle moved 360 km), releasing almost 830 kg of exhaust gases into the ionosphere (*6*). It was conducted after sunset in order to avoid simultaneous solar re-ionization of the atmosphere. The Millstone 1 experiment was thus designed to produce the largest and most long-lived ionospheric hole that might be caused by the shuttle. In contrast, the Millstone Hill 2 burn was conducted in mid-afternoon with a 6-second burn of a single OMS engine to release <10% of the molecules available for Millstone Hill 1 (68 kg) (*7*). Millstone 2 should help to define the lower limits of shuttle-induced ionospheric holes. In both cases, the OMS burns were placed south of the Millstone antenna in order to have the radar's ray path essentially parallel to the geomagnetic field lines, thereby maximizing the chance of measuring Doppler shifts from plasma diffusion along magnetic field lines into the depleted regions.

For the Hobart OMS burn, a different set of criteria prevailed. The goal of the experiment was to test the concept of conducting low-frequency radio astronomy through an artificially created ionospheric window (*8*). Cosmic radio signals in the 1- to 3-MHz band, synchrotron radiation from the interstellar medium, or discrete sources of planetary origin (for example, Jupiter's magnetosphere) are normally below the radio penetration frequency imposed by the ionospheric plasma. These signals are thus reflected back into space by the ionospheric electrons just as terrestrial signals in the same band are reflected back toward Earth, thereby making possible long-distance radio communication. The low-frequency radio observatory operated by the University of Tasmania in Hobart, Tasmania, Australia (42.30°S, 212.97°W), has conducted ground-based observations in the low-frequency domain from a site where the ionosphere is often naturally weak (the so-called mid-latitude trough). For the Spacelab-2 experiment, the OMS burn was conducted under near optimal conditions: predawn, winter-nighttime, solar minimum conditions, with the burn virtually above the antenna (*9*).

The large OMS burn across southern New England on the night of 29 July 1985 was monitored by a network of radio and optical diagnostic systems. During the subsequent burn of 4 August 1985, conducted in full daylight, observations were limited to the Millstone radar. Optical measurements (photometer and imaging systems) are used in ionospheric depletion experiments to record the 6300-Å airglow induced by the recombination chemistry that forms the hole. The red emission comes mainly from the CO_2 branch of the OMS-initiated chemistry. The dissociation of O_2^+ with electrons results in one or both of the oxgen atoms left in the ^1D state, with a radiative lifetime of 147 seconds. Optical emissions thereby map the recent occurrence of plasma depletions.

To observe the 6300-Å cloud emitted by the Millstone 1 shuttle burn, Boston University's Mobile Ionospheric Observatory (MIO) was deployed to Horton Point, Long Island, a site selected because of its proximity to the burn track and a forecast for clear skies there on the day of the experiment. Figure 1 shows the temporal pattern obtained with the 1° photometer in the MIO pointed to the center of the burn. Before the event, ambient airglow levels showed a gradual decline typical of summer post-sunset (2200 local time) ionospheric decay. Within seconds of the OMS burn, the 6300-Å signal increased sharply, reaching a maximum at ~2 minutes after the end of the OMS burn. The subsequent decay to pre-event levels took approximately 15 minutes. The airglow levels shown in Fig. 1 are well below the brightness levels required for visual observations. An image-intensified charge-coupled device (CCD) camera system can readily record such levels with an all-sky (fish-eye) lens (*10*). Figure 2 contains a summary of four images taken from the MIO on Horton Point that describe the spatial extent of the airglow cloud at the four times indicated on the photometer curve in Fig. 1. Although these images were taken from the ground, they have been transferred onto a geographic map by using an emission height corresponding to the shuttle's altitude (320 km) at the time of the burn. Also included on each frame are the OMS burn path, the MIO and Millstone Hill observation sites, the photometer monitoring point, and the ray path from the Millstone Radar, the latter two aimed at the burn center.

The images in Fig. 2 show an airglow cloud that begins as an elongated feature; these images reveal depletions formed by the OMS gases while they are still close to the shuttle trajectory. During the next few minutes, the effect spreads through the ionosphere as the molecules diffuse rapidly through the rarefied upper atmosphere. At the time of peak brightness [0325:02 universal time (UT)], the effect spans >300 km. In its later stages, the faint airglow cloud is nearly circular, covering ~400,000 km^2.

Several dynamic effects are evident in Fig. 2. The center of the airglow cloud is clearly displaced by ~150 km from the center of the OMS burn. This is due to the fact that the exhaust cloud shares in the shuttle's forward motion. With an orbital speed of ~8 km sec^{-1} toward the southeast, and the OMS exhaust gases at ~3 km sec^{-1} to the northwest, the molecules enter the ionosphere at ~5 km sec^{-1} in the direction of the shuttle's motion. Owing to the low atmospheric densities at 320 km altitude, $[O] = 1.3 \times 10^8$ cm^{-3} for a neutral temperature of 743 K (*11*), collisions occur at a frequency of ~0.1 sec^{-1}, and thus the forward motion of the cloud is stopped in about three collisions.

Figure 3 contains a summary of the changes in the electron density altitude profiles, $n_e(h)$, observed by the Millstone Hill radar during the formation stage of the hole. With the antenna pointed at elevation 56° and azimuth 179°, the beam crossed the shuttle altitude at the center of the burn. Note, therefore, that electron density values at altitudes <320 km come from regions below and to the north of the intersection point, whereas n_e for altitudes >320 km pertain to regions south of the intersection point. Individual electron density profiles were taken with a 20-second integration time and a pulse length of 48 km in slant range. Thus, the 1° beam of the antenna gives a 7 by 7 by 48 km^3 slice through the ionosphere at the range corresponding to the intersection point (~385 km). Because of the low signal-to-noise values associated with such an experiment, several individual profiles were averaged to give the mean evolution patterns shown in Fig. 3A.

During the first minute after the shuttle passed through the radar beam (Fig. 3B), one can see that a large depletion was readily detected. This ~45% hole in the local plasma density is flanked by small enhancements (~10%) above and below the core depletion. These enhancements are believed to be due to a physical displacement of plasma by the shuttle and its exhaust gases, the so-called "snowplow effect" associated with the injection of a dense gas into a plasma (*4, 12, 13*). This early-phase effect is quickly overpowered by recombination chemistry as the molecules begin to diffuse through the ionosphere. In Fig. 3C the hole is well formed, corresponding in time to the peak airglow production time in Figs. 1 and 2. In Fig. 3D, the hole is seen to recover somewhat at the center, to broaden in its altitude extent, and to have the peak depletions occur at lower altitudes. This pattern essentially marks the end of the rapid hole-making stage. Reacting to the strong gradients produced by the initial burst of chemistry, plasma now diffuses into the hole from above and below. Simultaneously, the heavy exhaust gases sink to lower ionospheric heights, causing further depletions. The airglow results show that this process continued for about 15 to 20 minutes.

Figure 3 also shows the electron density profile results obtained during the initial phase of the daytime Millstone burn. With the radar pointed at elevation 62° and azimuth 169°, and the burn placed to the west of the orbit-radar intersection point because of the slippage effect seen in Fig. 2, the resultant perturbations are seen to be remarkably similar in form, but reduced in magnitude, to the nighttime effects. The differences in depth can be related to the smallness of the burn and the replenishment of the ionosphere by solar ionizing radiation.

After the nighttime fixed-position observations shown in Fig. 3 were made, the Millstone radar conducted a series of elevation scans at the same azimuth in order to map the altitude-latitude extent of the hole.

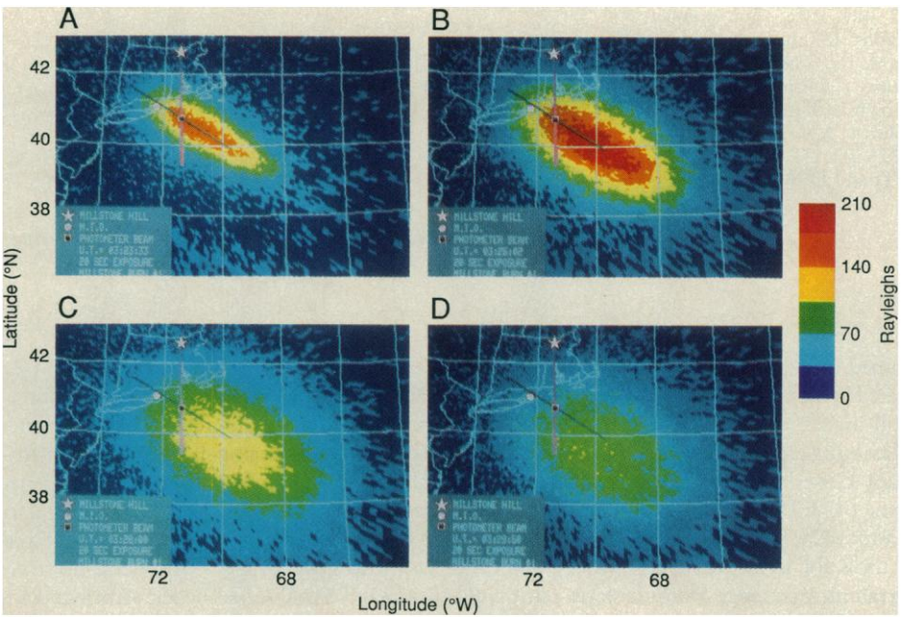

Fig. 2. Summary of four optical images (6300 Å) for the Millstone Hill nighttime experiment obtained with a CCD camera at Horton Point, Long Island. The optical emission comes from the neutralization of ionospheric ions and electrons caused by the CO_2 in the shuttle's exhaust. Each image is a 20-second exposure. The times of the images (as indicated on the photometer curve in Fig. 1) are (**A**) 0323:33 UT, (**B**) 0325:02 UT, (**C**) 0328:00 UT, and (**D**) 0329:50 UT. The photometer results in Fig. 1 give the induced 6300 Å on a background of ~40 rayleighs, but the images in this figure have the background levels subtracted. The symbols on the images indicate the following: star, the Millstone Hill site; circle, the MIO site; and square, the photometer monitoring point.

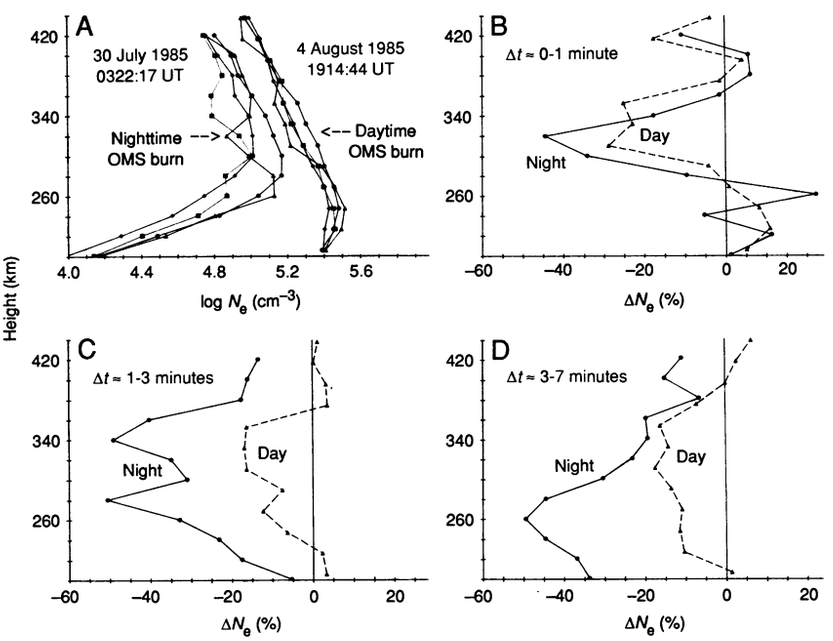

Fig. 3. Summary of early-time electron density variations observed by the Millstone Hill radar for both the night and day experiments. For the nighttime burn, the radar was held fixed at the elevation and azimuth corresponding to the center of the burn shown in Fig. 2. For the daytime experiment, the radar beam crossed the shuttle altitude at the elevation and azimuth corresponding to the end point of the OMS engine burn. (**A**) Nighttime and daytime electron density profiles; (**B**) electron density percentage differences during the first minute after the burns; (**C**) electron density percentage differences at 1 to 3 minutes after the burns; and (**D**) electron density percentage differences at 3 to 7 minutes after the burns.

Sample results from this mode give "late-time" effects that are shown in Fig. 4. The $n_e(h)$ versus latitude pattern seen in Fig. 4A is approximately 32 minutes before the experiment. The scan taken ~14 minutes after the burn (Fig. 4B) reveals a well-formed trough spanning about 1° of latitude. Forty minutes after the burn (Fig. 4C), a well-formed depletion duct continues to be observed. Observations in Fig. 4D, some 107 minutes after the burn, suggest a weak but lingering signature of the hole.

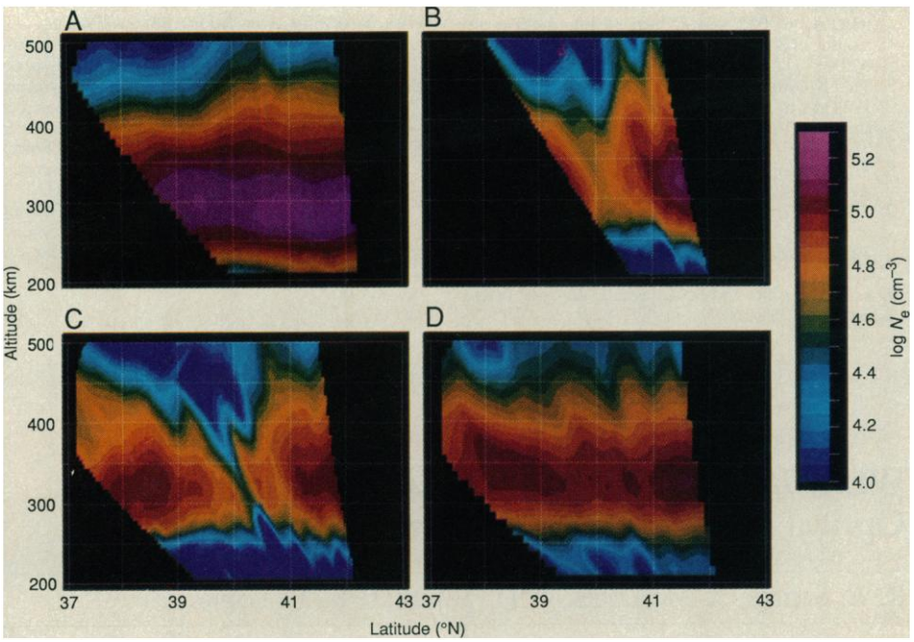

Fig. 4. Summary of the late-time electron density variations observed during the Millstone Hill nighttime experiment on 30 July 1985. The antenna was scanned in elevation angle to map the latitude-altitude structure of the hole. The panels show (**A**) conditions before the event (0247:41 to 0253:23 UT) and the resultant perturbations at (**B**) ~+14 minutes (0335:26 to 0338:56 UT), (**C**) ~+40 minutes (0359:19 to 0404:58 UT), and (**D**) ~+107 minutes (0506:47 to 0512:26 UT). The algorithm used to edit and smooth the radar observations tends to accentuate wavelike patterns in the raw data.

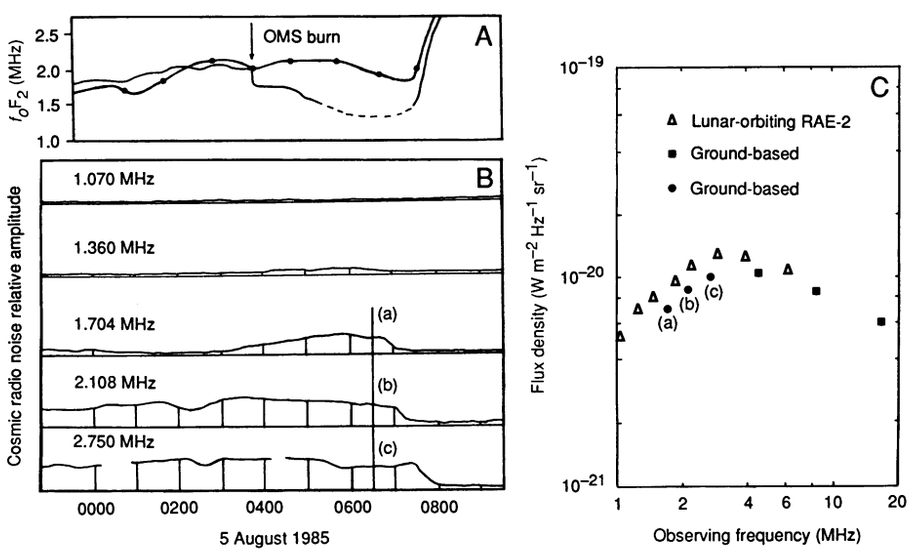

Fig. 5. (**A**) The behavior of the ionospheric penetration frequency (f_oF_2) recorded by an ionosonde in Hobart (solid and dashed line) and a control curve of hourly f_oF_2 values (filled circles) recorded in Melbourne (more than 500 km from the Hobart site). The dashed portion of the Hobart f_oF_2 curve from 0500 to 0700 UT expresses uncertainties in the very low f_oF_2 values. (**B**) Cosmic radio noise levels at various frequencies observed on the night of 5 August 1985 at the University of Tasmania Radio Observatory in Hobart. Times are in local time (LT), corresponding to UT plus 10 hours. (**C**) Galactic radio spectrum on a log frequency scale observed at 0630 LT (filled circles) by means of the observations at (a) 1.704 MHz, (b) 2.108 MHz, and (c) 2.750 MHz from (B). Additional ground-based observations (filled squares) at 4.7, 8.3, and 16.5 MHz are also shown (*19*). For comparison, the low-resolution spectrum observed by the lunar-orbiting spacecraft RAE-2 for the south galactic pole region is also shown (open triangles) (*18*).

A comparison of the airglow images in Fig. 2 and the latitude patterns in Fig. 4 points out that the radar scans did not cut through the exact center of the hole because of the exhaust slippage effect. The peak airglow brightness level in the images reached about 200 rayleighs (where 1 rayleigh is 10^6 photons per square centimeter per second), approximately 18% higher than the peak value seen where the photometer and radar were aimed. This relatively small difference in airglow would not be associated with additional depletions of comparable size. We thus believe that the radar data give a fairly accurate portrayal of the maximum size and depth of the ionospheric hole, in spite of the fact that the scan was not precisely through the hole center.

The images in Fig. 2 also suggest that the airglow cloud moved somewhat to the south (that is, in the last frame the line of symmetry is no longer along the burn trajectory). The radar data at late times (Fig. 4) do not show a significant displacement of the plasma hole. Such differences are probably related to the fact that atmospheric winds can move neutral species [for example, CO_2 and $O(^1D)$] horizontally (across magnetic field lines), whereas plasma is constrained to move essentially vertically (along the field lines).

To test the concept of opening a window for ground-based low-frequency radio astronomy, a 244-kg OMS burn was conducted over the University of Tasmania's radio observatory in Hobart. Pioneering efforts in low-frequency work have been conducted at that site during solar minimum years when the ionosphere is naturally weak (*14, 15*). The Spacelab-2 mission occurred during a period of very low solar activity, during a winter, predawn period in the Southern Hemisphere, conditions when the ionosphere is transparent to all but the lowest radio frequencies (f <2 MHz). The full set of diagnostic instruments and observations made during the Hobart experiment are described elsewhere (*16*).

After the shuttle engine burn, the F-region's peak electron density was reduced by approximately 30%, thereby lowering the penetration frequency (f_oF_2) from ~2.0 to ~1.7 MHz (Fig. 5A). Cosmic radio noise was monitored at a series of frequencies (1.070, 1.360, 1.704, 2.108, and 2.750 MHz) before and after the burn (Fig. 5B). The signals at 1.07 and 1.36 MHz remained unchanged since the electron densities in the depleted ionosphere were still too high to permit reception; at 2.1 and 2.8 MHz, the

received signals were unchanged since these frequencies were already above the penetration frequency. At 1.7 MHz, however, the transition occurred from no reception to reception. This is consistent with earlier observations that showed that the galactic signal normally begins leaking through the ionosphere when f_oF_2 falls to within about 100 kHz of the receiver frequency (*14*). The signal reached a maximum at 0540 hours and then slowly decreased until sunrise caused f_oF_2 to rise near 0700 hours. The profile from 0540 to 0640 hours was generally similar to that at 2.108 MHz and to the corresponding variation seen at the same right ascension in previous observations at 2.13 MHz (*17*) and may be taken to represent the galactic brightness distribution of declination −43° and right ascension of 0200 to 0300 hours. This is the first observation of this region at 1.7 MHz with 25° resolution, the nearest similar measurements having been made with the lunar-orbiting spacecraft RAE-2 at 1.3 MHz and with 130° resolution (*18*).

Figure 5C shows the spectrum of the galactic background radio emission derived from the observations at 0630 local time (galactic coordinates $\ell = 220°$, $b = -52°$). The spectrum observed by the RAE-2 spacecraft is shown for comparison. The flux measurement labeled (a) at 1.704 MHz represents the view through the "ionospheric hole" associated with the shuttle-induced plasma depletion. Observations over a period of several weeks before and after the experiment failed to produce any comparable records at 1.704 MHz since the natural ionospheric cutoff frequency never approached the low values associated with the Spacelab-2 "ionospheric hole" experiment.

The Millstone Hill experiments provided clear and unambiguous documentation of both the largest and smallest types of ionospheric holes capable of being induced by the space shuttle OMS engines. Although full modeling results are yet to be completed, the observations are essentially consistent with theories before the experiment. The sizes and longevities of the holes were somewhat larger and longer than anticipated, and the airglow patterns still require detailed simulation work to verify the dominant chemistry tracks. The dramatic slippage of the exhaust cloud through the ionosphere demonstrates the need for precise planning for future active experiments requiring gas releases at orbital speeds. In addition, the Hobart experiment succeeded in demonstrating that artificial means can be used to open ionospheric windows for the reception of low-frequency radiation of celestial origin.

REFERENCES AND NOTES

1. M. Mendillo and J. M. Forbes, *J. Geophys. Res.* **83**, 151 (1978).
2. P. A. Bernhardt, *ibid.* **84**, 793 and 4341 (1979).
3. M. Mendillo, *Adv. Space Res.* **1**, 275 (1981).
4. ———, *ibid.*, in press.
5. J. V. Evans, *Proc. IEEE* **57**, 496 (1969).
6. The Millstone 1 nighttime burn occurred from 0322:17 to 0323:04 UT on 30 July 1985 at an altitude of 320 km from 41.6°N, 73.1°W to 40.0°N, 69.8°W.
7. The Millstone 2 daytime burn occurred from 1914:44 to 1914:50 UT on 4 August 1985 at an altitude of 323 km from 40.9°N, 71.5°W to 41.1°N, 71.1°W.
8. M. D. Papagiannis and M. Mendillo, *Nature (London)* **255**, 42 (1975).
9. The Hobart burn occurred from 1659:27 to 1659:43 UT on 4 August 1985 at an altitude of 322 km from −42.4°N, 213.5°W to −42.9°N, 212.3°W.
10. J. Baumgardner and S. Karandanis, *Electron. Imaging* **3**, 28 (1984).
11. A. E. Hedin, *J. Geophys. Res.* **88**, 10170 (1983).
12. H. G. Booker, *ibid.* **66**, 1073 (1961).
13. R. H. Wand and M. Mendillo, *ibid.* **89**, 203 (1984).
14. G. Reber and G. R. A. Ellis, *ibid.* **61**, 1 (1956).
15. G. R. A. Ellis, *Mon. Notices R. Astron. Soc.* **130**, 429 (1965).
16. G. R. A. Ellis *et al.*, *Adv. Space Res.*, in press.
17. G. Reber, *J. Franklin Inst.* **285**, 1 (1967).
18. J. C. Novaco and L. W. Brown, *Astrophys. J.* **221**, 114 (1978).
19. G. R. A. Ellis, *Aust. J. Phys.* **35**, 91 (1982).

20. We thank the Spacelab-2 crew, NASA team members at the Marshall Space Fight Center (with special thanks to S. Perrine and the Orbital Dynamics Group), and many colleagues who contributed to these experiments. Funding for this work came in part from NASA contract NAS8-32844 to Boston University. The Millstone radar program was supported under NSF Cooperative Agreement ATM-84-19117 to the Massachusetts Institute of Technology. The University of Tasmania radio astronomy observations were financed by the Australian Research Grant Scheme.

26 May 1987; accepted 22 September 1987

White Light Sunspot Observations from the Solar Optical Universal Polarimeter on Spacelab-2

R. A. SHINE, A. M. TITLE, T. D. TARBELL, K. P. TOPKA

The flight of the Solar Optical Universal Polarimeter on Spacelab-2 provided the opportunity for the collection of time sequences of diffraction-limited (0.5 arc second) solar images with excellent pointing stability (0.003 arc second) and with freedom from the distortion that plagues ground-based images. A series of white-light images of active region 4682 were obtained on 5 August 1985, and the area containing the sunspot has been analyzed. These data have been digitally processed to remove noise and to separate waves from low-velocity material motions. The results include (i) proper motion measurements of a radial outflow in the photospheric granulation pattern just outside the penumbra; (ii) discovery of occasional bright structures ("streakers") that appear to be ejected outward from the penumbra; (iii) broad dark "clouds" moving outward in the penumbra, in addition to the well-known bright penumbral grains moving inward; (iv) apparent extensions and contractions of penumbral filaments over the photosphere; and (v) observation of a faint bubble or looplike structure that seems to expand from two bright penumbral filaments into the photosphere.

THE SOLAR OPTICAL UNIVERSAL POLARIMETER (SOUP) flew on the space shuttle Challenger as part of the Spacelab-2 mission from 29 July to 6 August 1985. A description of the SOUP instrument and a summary of the data obtained are given by Title *et al.* (*1*). Because of electronic and thermal problems, only the white-light film data were scientifically useful. However, the high resolution (approximately 0.5 arc sec or 350 km) and, more importantly, the stability and freedom from variable atmospheric distortion of these data have provided an unprecedented opportunity to study the dynamics of the solar photosphere by viewing and analyzing movie sequences.

The Spacelab-2 mission was flown during the sunspot minimum of the solar cycle, but we observed a medium-sized sunspot and a group of pores on the disk during the week of the mission. These features were in active region 4682, which was located at Carrington coordinates S15W30 during the SOUP observations. The region and the major sunspot were decaying. Images containing the sunspot in the field of view were obtained during portions of five orbits. The longest uninterrupted sequence was exposed during orbit 110 and consists of about 28 minutes of data with a frame taken every 2 seconds on 5 August 1985 between 1910 and 1938 Greenwich mean time. Analysis of data from the image stabilization system indicates a root mean square jitter of only

Lockheed Palo Alto Research Laboratory, Palo Alto, CA 94304.